Journal of Photochemistry, 14 (1980) 19 - 37

THE CHLORINE-ATOM-SENSITIZED OXIDATION OF CHLOROFORM

J. OLBREGTS

Chimie Physique Moléculaire, Faculté des Sciences, Université Libre de Bruxelles, 50, Ave F. D. Roosevelt, B.1050 Brussels (Belgium)

(Received October 8, 1979; in revised form March 11, 1980)

Summary

The chlorine-photosensitized oxidation of chloroform

$$CHCl_3 + \tfrac{1}{2}O_2 \rightarrow COCl_2 + HCl$$

was studied at 303, 346, 400 and 426 K. At the two higher temperatures the simultaneous oxygen-inhibited photochlorination

$$CHCl_3 + Cl_2 \rightarrow CCl_4 + HCl$$

was observed. The mechanism and kinetics of these reactions are discussed in detail and several complex rate constants are given concerning chain termination reactions and chain propagation reactions involving $Cl^{\cdot}$, $CCl_3^{\cdot}$ and $CCl_3O_2^{\cdot}$ radicals. The behaviour of this system is very similar to that of the chlorinated ethanes and ethylenes. Evidence for a chain termination reaction

$$CCl_3O_2^{\cdot} + Cl^{\cdot} \rightarrow \text{Products}$$

is given.

---

1. Introduction

In 1977 a paper [1] on the chlorine-atom-sensitized oxidation of chloroform was published; the importance of understanding the oxidation processes of this compound was emphasized with respect to the possible interaction of halocarbons with stratospheric ozone. However, a few months later Schumacher [2] commented on this paper and showed that its conclusions were not convincing. Therefore we undertook a detailed study of this system.

Similar studies have already been performed in our laboratory [3 - 10] and a general mechanism has been proposed [11] for the chlorine-photosensitized oxidation and the competitive oxygen-inhibited photochlorination of chloroethanes and chloroethylenes. This mechanism involves the formation of alkyl radicals $R^{\cdot}$ either by hydrogen atom abstraction by $Cl^{\cdot}$ radicals

$$RH + Cl^{\cdot} \xrightarrow{(2')} R^{\cdot} + HCl \qquad (I)$$

or by chlorine addition to a double bond

$$E + Cl^{\bullet} \xrightarrow{(2)} R^{\bullet} \tag{II}$$

followed by the reactions of this radical with chlorine or oxygen

$$\begin{aligned}
R^{\bullet} + Cl_2 &\xrightarrow{(3)} RCl + Cl^{\bullet} \\
R^{\bullet} + O_2 &\xrightarrow{(9)} RO_2^{\bullet} \\
RO_2^{\bullet} &\xrightarrow{(-9)} R^{\bullet} + O_2 \\
R^{\bullet} + RO_2^{\bullet} &\xrightarrow{(10)} RO_2R \\
RO_2^{\bullet} + RO_2^{\bullet} &\xrightarrow{(11)} RO_2R + O_2 \qquad \text{(III)} \\
RO_2^{\bullet} + RO_2^{\bullet} &\xrightarrow{(12)} 2RO^{\bullet} + O_2 \\
RO^{\bullet} &\xrightarrow{(13)} \text{Oxidation products + chain-propagating radicals} \\
RO^{\bullet} &\xrightarrow{(14)} \text{Chain-terminating step}
\end{aligned}$$

Long-chain oxidation (corresponding to $v_{13} \gg v_{14}$) has been observed for systems for which reactions (9) and (—9) are in equilibrium; the rates of these oxidation reactions are given by

$$v_{Ox} = I_a[O_2]/(k_{10}k_{-9}/2k_{12}k_9 + k_{11}[O_2]/2k_{12}) \tag{IV}$$

This means that under these conditions no dependence on substrate concentration is observed. Chloroform appears to behave differently; Schumacher and Wolff [12] have observed that the rate of oxidation

$$CHCl_3 + \tfrac{1}{2}O_2 \rightarrow COCl_2 + HCl \tag{V}$$

depends on the square root of the concentration of chloroform. Sanhueza [1] also states that "the quantum yields for the consumption of $CHCl_3$ and for the production of $COCl_2$ increased with the $CHCl_3$ pressure, approaching an upper limiting value of 200". He suggests that this chloroform dependence should be explained by a three-body recombination of chlorine atoms

$$Cl^{\bullet} + Cl^{\bullet} + M \xrightarrow{(6)} Cl_2 + M \tag{VI}$$

The experimental data to support this assumption are rather poor [2], and it is clear that it is not possible to obtain the value $k_2'/k_6{}^{1/2} = 100\ s^{-1/2}$ [1]

from these data. Indeed, considering both the chain termination reactions (6) and (11) and assuming steady state conditions and long chains, the rate equation obtained is

$$\Phi = v_{Ox}/I_a$$

$$= (2k_{12}/k_{11}) - (2k_6k_{12}/k_{11}k_2'^2)([M]v_{Ox}^2/I_a[CHCl_3]^2) \qquad (VII)$$

A plot of Φ against $[M]v_{Ox}^2/I_a[CHCl_3]^2$ for the data of Sanhueza shows a large scatter of experimental points but yields no reliable slope.

In a previous paper Huybrechts *et al.* [6] have suggested that the observed lower value of the oxidation rate of C_2HCl_5 compared with that of C_2Cl_4 could result from the additional chain-terminating step

$$RO_2^{\cdot} + Cl^{\cdot} \xrightarrow{(16)} \text{Products} \qquad (VIII)$$

and have found evidence for this step in some preliminary results on the chlorine-photosensitized oxidation of chloroform. It would be interesting to compare the relative importance of the terminating steps (6), (11) and (16) in that system. In the long-chain oxidation, when inhibited photochlorination is negligible, the chain-propagating steps (2′), (12) and (13) all have the same rate, which is equal to the observed oxidation rate; therefore

$$[Cl^{\cdot}] = v_{Ox}/k_2'[CHCl_3] \qquad (IX)$$

and

$$[CCl_3O_2^{\cdot}] = (v_{Ox}/2k_{12})^{1/2} \qquad (X)$$

and also

$$[CCl_3O_2^{\cdot}]/[Cl^{\cdot}] = k_2'[CHCl_3]/(v_{Ox}2k_{12})^{1/2} \qquad (XI)$$

Taking eqn. (XI) into account, the rates of the terminating steps are given by

$$v_6 = k_6[M][Cl^{\cdot}]^2 \qquad (XII)$$

$$v_{11} = (k_{11}k_2'^2[CHCl_3]/2k_{12}v_{Ox})[Cl^{\cdot}]^2 \qquad (XIII)$$

and

$$v_{16} = \{k_{16}k_2'[CHCl_3]/(2k_{12}v_{Ox})^{1/2}\}[Cl^{\cdot}]^2 \qquad (XIV)$$

From the known value of k_2' [13], the highest proposed value for k_6 [14], the value for $2k_{12}/k_{11}$ of 200 obtained from the maximum quantum yield of oxidation [1] and the lowest experimental values of $[CHCl_3]/v_{Ox}^{1/2}$ [1], it can be calculated that

$$v_6/v_{11} \leqslant 4 \times 10^{-3} \qquad (XV)$$

and

$$v_{16}/v_{11} \leqslant 10^{-6}k_{16}/k_{11}^{1/2} \qquad (XVI)$$

These equations clearly show that, under the experimental conditions used by Sanhueza [1], it will never be possible to observe the chain-terminating step (6). In contrast, assuming reasonable values for the bimolecular radical recombination rate constants k_{11} and k_{16}, a contribution from the chain-terminating step (16) cannot be excluded; eqns. (XIII) and (XIV) indicate that the ratio v_{16}/v_{11} increases with increasing values of v_{Ox} (*i.e.* with increasing values of the absorbed light intensity) and with decreasing values of chloroform concentration. Taking this into account, it seems interesting to undertake a systematic study of the chlorine-photosensitized oxidation of chloroform to establish properly a mechanism that accounts for the chloroform dependence previously observed [1, 12]; this is the aim of the present work.

2. Experimental

2.1. *Procedures*

The experimental procedure has already been described [4, 6]. A cylindrical Pyrex reactor (length, 11.9 cm; diameter, 3.9 cm) was equipped with a spoon gauge to measure the total pressure. The chlorine partial pressure was measured photometrically at about 350 nm (obtained from an incandescent lamp provided with an 18A Kodak filter) using a logarithmic photometer [15]. The actinic light at 436 nm was obtained from a mercury lamp (Philora HP 125) provided with a blue filter (Kodak Wratten 47) [16]. The light intensity was measured using the photochlorination of trichloroethylene as an actinometer [16].

2.2. *Reactants*

Commercial tank chlorine (Solvay)* was purified as described earlier [4]. Carbon dioxide present as an impurity in the chlorine was eliminated by distilling the chlorine through a trap cooled at the melting point of ethanol (161 K). Chloroform* was washed several times with water and was dried using molecular sieves. The only impurities detected were 1,1-dichloroethane (56 ppm) and chlorobromomethane (<50 ppm).

3. Results

The chlorine-photosensitized oxidation of chloroform was studied at 303, 346, 400 and 426 K. The stoichiometry of the reaction has been established previously [1, 12]:

$$CHCl_3 + \tfrac{1}{2}O_2 \rightarrow COCl_2 + HCl \qquad \text{(XVII)}$$

---

*Solvay Research Center kindly supplied us with these products.

Some experiments were performed at 303 and 346 K to check this stoichiometry. After irradiation of mixtures of $CHCl_3$, O_2 and Cl_2, the reaction products were separated [7] into four fractions: (1) condensable at 195 K (dry ice); (2) condensable at 142 K (melting point of *n*-pentane); (3) condensable at 78 K (liquid nitrogen); (4) non-condensable at 78 K. The first fraction was analysed by gas chromatography and contained the unreacted $CHCl_3$ and its chlorination product CCl_4. The second fraction was passed over a column of $SbCl_3$ to eliminate the unreacted chlorine. The residual was identified as $COCl_2$ and was titrated by iodometry [17]. The third fraction consisted of HCl; it was dissolved in an excess of NaOH which was then titrated using oxalic acid. The fourth fraction was the unreacted oxygen. These analyses showed that the change in total pressure P_{tot} corresponded to half the pressure of $COCl_2$ formed, in agreement with eqn. (XVII). In the kinetic study the rate of oxidation was thus taken as

$$v_{Ox} = (2/RT)\mathrm{d}P_{tot}/\mathrm{d}t$$

At the higher temperatures (400 and 426 K) the oxygen-inhibited photochlorination

$$CHCl_3 + Cl_2 \rightarrow CCl_4 + HCl$$

was also observed. The rate of this reaction was obtained from the variation of the partial pressure of chlorine:

$$v_{Cl} = -(1/RT)\mathrm{d}P_{Cl_2}/\mathrm{d}t$$

The experimental conditions are given in Table 1. At 303 and 346 K the inhibited photochlorination was always negligible compared with the oxidation. At 400 K both reactions were observed with comparable rates, while at 426 K the oxidation was generally slower than the chlorination. The reaction orders with respect to the absorbed light intensity I_a and to the Cl_2, O_2 and $CHCl_3$ concentrations were determined under initial conditions; typical results for these determinations are given in Tables 2 - 5. The oxidation is first order with respect to the absorbed light intensity and zero order with respect to the chlorine concentration, while the rate of the inhibited chlorination depends on the square root of the absorbed light intensity and

TABLE 1

Experimental conditions

T (K)	*Number of experiments*	$I_0 \times 10^{10}$ (einstein l^{-1} s^{-1})	P_{Cl_2} (Torr)	P_{CHCl_3} (Torr)	P_{O_2} (Torr)	P_{tot} (Torr)
303	49	16 - 150	20 - 200	3 - 200	1 - 300	72 - 500
346	29	13 - 440	20 - 200	5 - 300	6 - 300	140 - 500
400	24	6.8 - 72	20 - 200	10 - 300	20 - 300	130 - 560[a]
426	15	78	60 - 210	6 - 200	20 - 210	180 - 550

[a] 100 - 400 Torr N_2 were added to five experiments.

TABLE 2

Chlorine-photosensitized oxidation and oxygen-inhibited photochlorination of chloroform: initial rates against absorbed light intensity

T (K)	P_{CHCl_3} (Torr)	P_{Cl_2} (Torr)	P_{O_2} (Torr)	$I_a \times 10^9$ (einstein l^{-1} s^{-1})	$v_{Ox} \times 10^7$ (mol l^{-1} s^{-1})	$v_{Cl} \times 10^7$ (mol l^{-1} s^{-1})
303	20.3	199.1	50.0	2.10	9.54	
	20.1	199.8	50.1	0.667	2.83	
	20.6	199.4	50.4	6.17	29.0	
346	20.4	101.1	103.8	3.04	13.1	
	20.2	100.3	105.5	2.79	15.3	
	20.4	99.2	106.4	9.47	60.5	
	21.2	103.2	106.1	0.98	7.60	
	20.4	99.9	104.5	0.28	1.90	
400	100.3	101.5	96.9	1.48	18.2	4.55
	99.9	99.4	99.6	0.404	3.88	2.41
	99.9	99.1	99.5	0.138	1.00	1.47

TABLE 3

Chlorine-photosensitized oxidation and oxygen-inhibited photochlorination of chloroform: initial rates against partial pressure of chlorine

T (K)	P_{CHCl_3} (Torr)	P_{Cl_2} (Torr)	P_{O_2} (Torr)	$I_a \times 10^9$ (einstein l^{-1} s^{-1})	v_{Ox}/I_a	$10^2 v_{Cl}/I_a^{1/2}$[a] (mol$^{1/2}$ $l^{-1/2}$ $s^{-1/2}$)
303	20.0	100.1	99.9	1.23	474	
	20.1	50.0	100.0	0.667	397	
	20.0	199.9	100.0	2.22	477	
	19.9	100.0	101.0	1.23	488	
346	100.1	101.2	105.2	3.10	766	
	100.2	201.2	105.0	5.55	863	
	100.3	21.1	105.0	0.685	861	
	100.0	50.4	104.7	1.56	916	
400	100.3	101.5	96.9	1.48	1230	1.2
	102.2	201.9	98.1	1.51	1170	2.3
	99.3	20.4	99.7	0.322	1250	0.2
426	194.5	162.2	194.1	2.38		5.39
	191.1	62.8	194.0	1.02		1.95

[a] The order with respect to I_a was taken into account to eliminate the dependence of chlorine concentration contained in I_a.

on the first power of the chlorine concentration. The dependences on oxygen and chloroform concentrations are more complicated. At 303 and 346 K no significant variation of the rate of oxidation is observed for oxygen pressures ranging from 1 to 200 Torr and from 20 to 200 Torr respectively. At 400 K

TABLE 4

Chlorine-photosensitized oxidation and oxygen-inhibited photochlorination of chloroform: initial rates against partial pressure of oxygen

T (K)	P_{CHCl_3} (Torr)	P_{Cl_2} (Torr)	P_{O_2} (Torr)	$I_a \times 10^9$ (einstein l^{-1} s^{-1})	$v_{Ox} \times 10^7$ (mol l^{-1} s^{-1})	$v_{Cl} \times 10^7$ (mol l^{-1} s^{-1})
303	59.9	63.1	20.0	1.37	6.0	
	60.1	60.0	63.8	1.31	6.2	
	59.9	60.2	205.1	1.32	6.9	
	60.2	62.3	60.3	1.25	6.6	
	60.4	59.9	6.3	1.20	7.3	
	60.2	60.4	6.0	1.24	7.8	
	60.0	59.9	200.1	1.20	8.7	
	60.2	60.9	0.9	1.20	7.0	
346	100.1	101.2	105.2	3.10	24.4	
	99.9	100.8	300.0	3.06	27.2	
	95.0	100.8	20.7	3.12	26.6	
400	100.3	101.5	96.9	1.48	18.2	4.55
	99.7	100.1	20.0	1.46	8.2	11.3
	99.9	99.4	199.5	1.45	17.7	1.80
426	193.7	133.2	20.5	1.95		43.4
	196.8	133.2	73.2	2.06		33.7
	195.3	133.2	–	2.01		46.8

the rate of oxidation increases with increasing oxygen pressure up to a limiting value obtained for oxygen pressures higher than 100 Torr. The rate of the simultaneous inhibited photochlorination decreases with increasing oxygen pressures following an $[O_2]^{-n}$ dependence with n close to $\frac{1}{2}$ for low oxygen pressures. At 426 K the sensitivity of the chlorination to the inhibiting effect of oxygen is rather small; the rate decreases by less than 10% for oxygen pressures of 20 Torr. Finally, the rate of oxidation does not depend on the chloroform concentration for high concentrations and depends on $[CHCl_3]^{1/2}$ for low concentrations; the limit between low and high concentrations lies at about 50 Torr. The rate of the inhibited chlorination also depends in this way on the chloroform concentration.

For some experiments a dark reaction with a very small rate was observed after the cut-off of the actinic light. Such an "after effect" has already been observed and explained in other systems [3, 6, 10]. In the case of chloroform, this effect is too small to be described quantitatively.

4. Discussion

4.1. Data at 303, 346 and 400 K

The results at 303, 346 and 400 K for the higher chloroform pressures can be explained by the following mechanism:

TABLE 5

Chlorine-photosensitized oxidation and oxygen-inhibited photochlorination of chloroform: initial rates against partial pressure of chloroform

T (K)	P_{CHCl_3} (Torr)	P_{Cl_2} (Torr)	P_{O_2} (Torr)	$I_a \times 10^9$ (einstein l^{-1} s^{-1})	$v_{Ox} \times 10^7$ (mol l^{-1} s^{-1})	$v_{Cl} \times 10^7$ (mol l^{-1} s^{-1})
303	195.0	99.8	100.2	1.31	7.1	
	176.4	99.7	99.8	1.27	6.7	
	53.8	100.6	99.9	1.29	7.2	
	9.9	100.0	100.2	1.27	4.2	
	5.2	99.9	99.9	1.27	3.5	
	3.1	100.7	100.2	1.31	3.0	
346	159.8	100.8	104.0	3.15	30.2	
	40.0	100.7	104.2	3.12	18.6	
	300.2	101.0	104.0	3.21	35.3	
	9.6	100.6	104.8	2.83	11.1	
	4.7	100.4	104.8	2.79	5.6	
400	99.7	100.1	20.0	1.46	8.2	11.3
	10.0	99.7	20.0	1.36	6.7	9.0
	304.0	100.1	20.0	1.32	10.3	14.3
	9.6	99.8	20.0	1.34	7.0	9.1
426	191.1	82.8	194.0	1.02		6.2
	19.8	62.4	187.1	1.04		3.3

$$
\begin{array}{lll}
Cl_2 & \rightarrow 2Cl^{\bullet} & I_a \\
Cl^{\bullet} + CHCl_3 & \xrightarrow{(2')} CCl_3^{\bullet} + HCl & k'_2 \\
CCl_3^{\bullet} + Cl_2 & \xrightarrow{(3)} CCl_4 + Cl^{\bullet} & k_3 \\
CCl_3^{\bullet} + O_2 & \underset{(-9)}{\overset{(9)}{\rightleftarrows}} CCl_3O_2^{\bullet} & k_9,\ k_{-9} \\
CCl_3O_2^{\bullet} + CCl_3^{\bullet} & \xrightarrow{(10)} CCl_3O_2CCl_3 & k_{10} \\
2CCl_3O_2^{\bullet} & \xrightarrow{(11)} CCl_3O_2CCl_3 + O_2 & k_{11} \\
2CCl_3O_2^{\bullet} & \xrightarrow{(12)} 2CCl_3O^{\bullet} + O_2 & k_{12} \\
CCl_3O^{\bullet} & \xrightarrow{(13)} COCl_2 + Cl^{\bullet} & k_{13}
\end{array}
\qquad \text{(XVIII)}
$$

Assuming constancy for the radical concentrations and complete reversibility of reaction (9) (*i.e.* $v_9 = v_{-9}$), this mechanism leads to

$$v_{\mathrm{Cl}} = k_3[\mathrm{Cl}_2]I_a^{1/2}/\{(k_{10}k_9/k_{-9})[\mathrm{O}_2] + (k_{11}k_9^2/k_{-9}^2)[\mathrm{O}_2]^2\}^{1/2} \qquad \text{(XIX)}$$

and

$$v_{\mathrm{Ox}} = 2k_{12}I_a/\{(k_{10}k_{-9}/k_9)/[\mathrm{O}_2] + k_{11}\} \qquad \text{(XX)}$$

These equations can be linearized by writing

$$I_a[\mathrm{Cl}_2]^2/v_{\mathrm{Cl}}^2[\mathrm{O}_2] = k_{10}k_9/k_3^2k_{-9} + (k_{11}k_9^2/k_3^2k_{-9}^2)[\mathrm{O}_2] \qquad \text{(XXI)}$$

and

$$I_a/v_{\mathrm{Ox}} = k_{11}/2k_{12} + (k_{10}k_{-9}/2k_{12}k_9)[\mathrm{O}_2]^{-1} \qquad \text{(XXII)}$$

The data for experiments at $P_{\mathrm{CHCl}_3} > 100$ Torr were plotted according to eqns. (XXI) and (XXII) (Figs. 1 and 2). It must be emphasized that, given the very large range of experimental conditions and the cumulated experimental uncertainties on these complicated functions (mainly for $I_a[\mathrm{Cl}_2]^2/v_{\mathrm{Cl}}^2[\mathrm{O}_2]$), the compatibility of the data with a linear function is rather good. Nevertheless, it is obvious that these figures alone are not sufficient to prove the validity of the proposed mechanism. Moreover, the important scatter probably indicates that some additional reaction steps of minor importance should be introduced into the mechanism.

The intercept and slope of the straight line drawn through the experimental points of Fig. 1 lead to the following estimates at 400 K:

$$k_{10}k_9/k_3^2k_{-9} = 10 \text{ s} \qquad \text{(XXIII)}$$

$$k_{11}k_9^2/k_3^2k_{-9}^2 = 6 \times 10^3 \text{ mol}^{-1} \text{ l s} \qquad \text{(XXIV)}$$

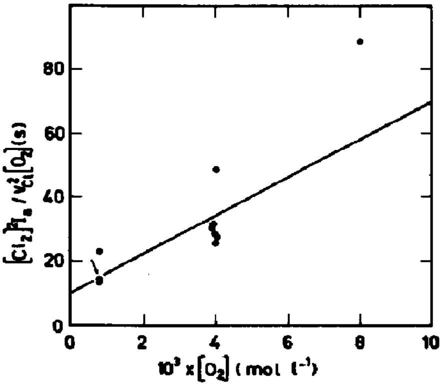

Fig. 1. The oxygen-inhibited photochlorination of chloroform at 400 K (see eqn. (XXI)). Experimental conditions: pressure (Torr), $99.3 < P_{\mathrm{CHCl}_3} < 304.0$, $20.4 < P_{\mathrm{Cl}_2} < 201.9$, $20.0 < P_{\mathrm{O}_2} < 199.5$; incident light intensity (einstein $\mathrm{l}^{-1}\,\mathrm{s}^{-1}$), $6.85 \times 10^{-10} < I_0 < 7.18 \times 10^{-9}$. The arrow indicates an experiment with 203.6 Torr N_2 added.

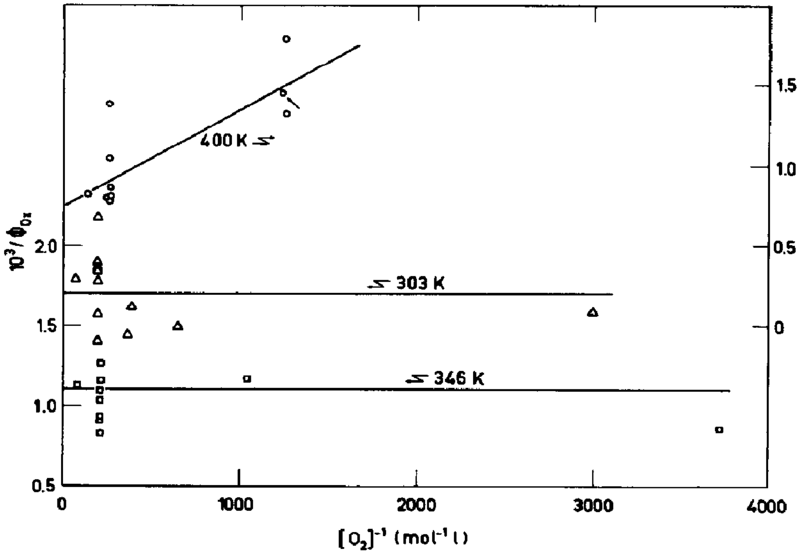

Fig. 2. The chlorine-photosensitized oxidation of chloroform at 303 (△), 346 (□) and 400 K (○). (Φ_{Ox} is the quantum yield of oxidation.) Experimental conditions (pressures (Torr), incident light intensity (einstein l^{-1} s^{-1})): 303 K, $99.8 < P_{CHCl_3} < 195.0$, $19.5 < P_{Cl_2} < 200.0$, $6.3 < P_{O_2} < 299.8$, $1.65 \times 10^{-9} < I_0 < 5.87 \times 10^{-9}$; 346 K, $95.0 < P_{CHCl_3} < 300.2$, $21.1 < P_{Cl_2} < 201.2$, $5.8 < P_{O_2} < 300.0$, $1.23 \times 10^{-8} < I_0 < 1.47 \times 10^{-8}$; 400 K, see the caption to Fig. 1.

Using the known value [18]

$$\log_{10} k_3 \ (\text{l mol}^{-1} \ \text{s}^{-1}) = 8.74 - 5000/4.58T \qquad \text{(XXV)}$$

the following can be obtained:

$$k_{10}k_9/k_{-9} = 1 \times 10^{13} \ \text{mol}^{-2} \ \text{l}^2 \ \text{s}^{-1} \qquad \text{(XXVI)}$$

and

$$k_{11}k_9^2/k_{-9}^2 = 6 \times 10^{15} \ \text{mol}^{-3} \ \text{l}^3 \ \text{s}^{-1} \qquad \text{(XXVII)}$$

These estimates must be correct to within a factor of two for verification of the mechanism at this stage.

Figure 2 shows no measurable slope at 303 K or at 346 K. This means that

$$k_{10}k_{-9}/k_{12}k_9 < 2 \times 10^{-7} \ \text{mol l}^{-1} \qquad \text{(XXVIII)}$$

at these temperatures.

An estimate of

$$k_{10}k_{-9}/k_{12}k_9 = 1.2 \times 10^{-6} \ \text{mol l}^{-1} \qquad \text{(XXIX)}$$

can be proposed from the slope of the data at 400 K. The intercepts lead to

$$k_{11}/k_{12} = 3.4 \times 10^{-3}, \ 2.2 \times 10^{-3} \ \text{and} \ 1.5 \times 10^{-3} \qquad \text{(XXX)}$$

respectively at 303, 346 and 400 K.

By combining eqns. (XXIX) and (XXX)

$$k_{10}k_{-9}/k_{11}k_9 = 8 \times 10^{-4}\ \mathrm{mol\ l^{-1}} \qquad \text{(XXXI)}$$

is obtained, while eqns. (XXIII) and (XXIV) yield for the same complex constant at the same temperature

$$k_{10}k_{-9}/k_{11}k_9 = 17 \times 10^{-4}\ \mathrm{mol\ l^{-1}} \qquad \text{(XXXII)}$$

The agreement between the values (eqns. (XXXI) and (XXXII)) obtained from independent experimental data (v_{Cl} and v_{Ox}) is within a factor of two, *i.e.* less than the combined uncertainties on these values. This argument gives support to the proposed mechanism. Even if the scatter of the experimental points in Figs. 1 and 2 may be partly explained by the experimental errors, it is clear that mechanism (XVIII) is not complete; this is evident from the observed dependence of the rates on the chloroform concentration observed at $P_{CHCl_3} < 100$ Torr. As we pointed out in Section 1, a chain-terminating step which has been suggested previously(16)

$$CCl_3O_2^{\cdot} + Cl^{\cdot} \rightarrow \text{Products} \qquad k_{16} \qquad \text{(XXXIII)}$$

can probably explain the present experimental data.

A reaction mechanism consisting of the steps of scheme (XVIII) and reaction (16) (see eqn. (XXXIII)) leads to very complicated rate equations. The steady state concentration of radicals cannot be expressed simply as a function of reactant concentration or of absorbed light intensity. Therefore, in the general stationary state equation

$$I_a = k_{10}[CCl_3O_2^{\cdot}][CCl_3^{\cdot}] + k_{11}[CCl_3O_2^{\cdot}]^2 + k_{16}[CCl_3O_2^{\cdot}][Cl^{\cdot}] \qquad \text{(XXXIV)}$$

we will express the radical concentrations as functions of the rates of oxidation and chlorination, *i.e.*

$$[CCl_3^{\cdot}] = v_{Cl}/k_3[Cl_2] \qquad \text{(XXXV)}$$

$$[CCl_3O_2^{\cdot}] = (v_{Ox}/2k_{12})^{1/2} \qquad \text{(XXXVI)}$$

and given the long chains

$$[Cl^{\cdot}] = (v_{Cl} + v_{Ox})/k_2'[CHCl_3] \qquad \text{(XXXVII)}$$

Equations (XXXIV) - (XXXVII) yield

$$I_a/v_{Ox} = \{k_{10}/k_3(2k_{12})^{1/2}\}v_{Cl}/[Cl_2]\,v_{Ox}{}^{1/2} + k_{11}/2k_{12} + \\ + \{k_{16}/k_2'(2k_{12})^{1/2}\}(v_{Ox}{}^{1/2}/[CHCl_3])(v_{Cl} + v_{Ox})/v_{Ox} \qquad \text{(XXXVIII)}$$

At 303 and 346 K no measurable chlorination was observed. This means that the contribution of the chain-terminating step (10) (the first term in eqn. (XXXVIII)) is negligible. This was already observed from the absence of a measurable slope in Fig. 2 in the interpretation of the experiments with $P_{CHCl_3} > 100$ Torr. A plot of the inverse of the quantum yield of oxidation

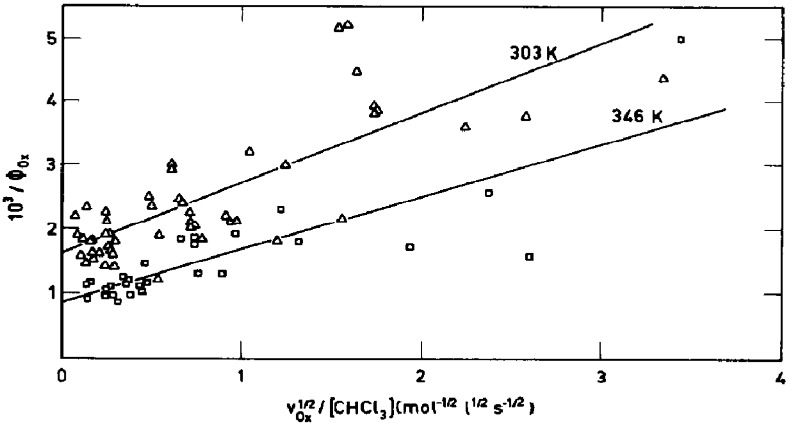

Fig. 3. The oxidation of chloroform at 303 (△) and 346 K (□). (The experimental conditions are given in Table 1.)

I_a/v_{Ox} against $v_{Ox}{}^{1/2}/[CHCl_3]$ is given in Fig. 3 for all the experiments at 303 and 346 K. The intercepts and slopes calculated by linear regression yield

$$k_{11}/k_{12} = 3.2 \times 10^{-3} \text{ and } 1.7 \times 10^{-3} \qquad \text{(XXXIX)}$$

and

$$k_{16}/k_2'(2k_{12})^{1/2} = 10.9 \times 10^{-4} \text{ and } 8.2 \times 10^{-4} \text{ mol}^{1/2}\ \text{l}^{-1/2}\ \text{s}^{1/2} \qquad \text{(XXXX)}$$

at 303 and 346 K respectively.

Using the known value of k_2' [13]

$$\log_{10} k_2' \ (\text{mol}^{-1}\ \text{l}\ \text{s}^{-1}) = -3350/4.58T + 9.84 \qquad \text{(XXXXI)}$$

the values

$$k_{16}/k_{12}{}^{1/2} = 4.1 \times 10^4 \text{ and } 6.1 \times 10^4 \text{ mol}^{-1/2}\ \text{l}^{1/2}\ \text{s}^{-1/2} \qquad \text{(XXXXII)}$$

are obtained at these temperatures.

At 400 K the chlorination rate is no longer negligible; all the terms in eqn. (XXXVIII) must be taken into account. A value of

$$k_{10}/k_3(2k_{12})^{1/2} = 3.5 \times 10^{-3} \text{ mol}^{1/2}\ \text{l}^{-1/2}\ \text{s}^{1/2}$$

can be estimated from eqns. (XXIII), (XXIV) and (XXX) and the k_{10} term in eqn. (XXXVIII) can be introduced as a correction for the inverse of the oxidation quantum yield. This yields the plot shown in Fig. 4. Seven experiments for which the correction term (*i.e.* the k_{10}-containing term) was larger than $0.5I_a/v_{Ox}$ were not taken into account in this plot. The intercept and slope calculated by linear regression yield at 400 K

$$k_{11}/k_{12} = 1.3 \times 10^{-3} \qquad \text{(XXXXIII)}$$

and

$$k_{16}/k_2'(2k_{12})^{1/2} = 3.1 \times 10^{-4} \text{ mol}^{1/2}\ \text{l}^{-1/2}\ \text{s}^{1/2} \qquad \text{(XXXXIV)}$$

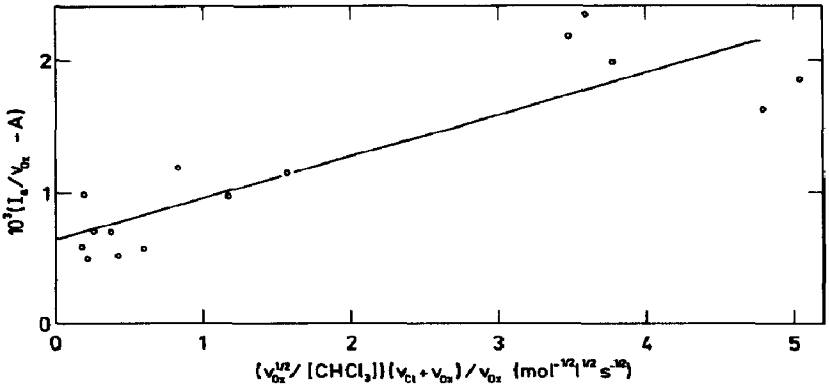

Fig. 4. The oxidation of chloroform at 400 K: $A = \{k_{10}/k_3(2k_{12})^{1/2}\}v_{Cl}/[CHCl_3]v_{Ox}^{1/2}$.

and thus from the value of k_2' [13] (see eqn. (XXXXI))

$$k_{16}/k_{12}^{1/2} = 4.5 \times 10^4 \text{ mol}^{-1/2} \text{ l}^{1/2} \text{ s}^{-1/2} \qquad \text{(XXXXV)}$$

The values obtained at 303, 346 and 400 K for the ratio k_{11}/k_{12} are of the same order of magnitude as for other systems (see for example CCl_3CH_2Cl [10], C_2HCl_3 [5], C_2HCl_5 and C_2Cl_4 [6]). The constant $k_{16}/k_{12}^{1/2}$ involves no measurable activation energy. Both constants k_{12} and k_{16} concern bimolecular radical–radical reactions, the values of which are generally about 10^8 - 10^{11} mol^{-1} l s^{-1}; therefore the observed value of $k_{16}/k_{12}^{1/2}$ is quite reasonable.

The complicated kinetics of this system do not permit simple linear plots of the experimental data to be obtained. All the figures given in this interpretation present significant scatter so that none of them, taken alone, definitely demonstrates the validity of the proposed mechanism. However, the interpretation of the independent experimental data on chlorination and oxidation, or the interpretation of the combined data, are all consistent with each other and with observations on other similar systems.

The observations at 303, 346 and 400 K can be summarized as follows: because of the very low value of k_{-9}/k_9 at 303 and 346 K, the ratio $[R^\cdot]/[RO_2^\cdot]$ is very small and therefore neither chlorination nor $R^\cdot + RO_2^\cdot$ chain termination is observed. Under these conditions the chain termination $RO_2^\cdot + RO_2^\cdot$ is dominant and the importance of the chain termination $RO_2^\cdot + Cl^\cdot$ increases with decreasing values of P_{CHCl_3}. At 400 K the ratio k_{-9}/k_9 becomes high enough to have non-negligible concentrations of radicals which are responsible for the chlorination and the observation of chain termination [10].

4.2. *Inhibited photochlorination data at 426 K*

At this temperature the oxidation becomes rather unimportant compared with the inhibited chlorination. The inhibiting effect of oxygen on the photochlorination is very small (see Table 4); this means that the chain terminations

$$\begin{aligned} CCl_3^{\cdot} + Cl^{\cdot} &\xrightarrow{(7)} CCl_4 \\ CCl_3^{\cdot} + CCl_3^{\cdot} &\xrightarrow{(8)} C_2Cl_6 \end{aligned} \qquad \text{(XXXXVI)}$$

characteristic of the uninhibited reaction are not negligible. Taking into account reaction scheme (XVIII) with the additional steps (7) and (8) (see eqns. (XXXXVI)) for the experiments in which the oxidation is negligible ($v_{Ox} < 0.2v_{Cl}$), the following rate equation is obtained:

$$v_{Cl} = k_3[Cl_2]I_a^{1/2}/(k_7k_3[Cl_2]/k_2'[CHCl_3] + k_8 + k_{10}k_9[O_2]/k_{-9} + + k_{11}k_9^2[O_2]^2/k_{-9}^2)^{1/2} \qquad \text{(XXXXVII)}$$

or

$$I_a[Cl_2]^2/v_{Cl}^2 = (k_7/k_3k_2')[Cl_2]/[CHCl_3] + k_8/k_3^2 + + (k_{10}k_9/k_{-9}k_3^2)[O_2] + + (k_{11}k_9^2/k_3^2k_{-9}^2)[O_2]^2 \qquad \text{(XXXXVIII)}$$

At 426 K k_7/k_3k_2' is about six times smaller than k_8/k_3^2 [18] and thus $k_t/k_3^2 = (k_7/k_3k_2')[Cl_2]/[CHCl_3] + k_8/k_3^2$ is almost constant for all values of $[Cl_2]/[CHCl_3]$ less than unity. The experimental data for $P_{CHCl_3} > 150$ Torr and $P_{O_2} < 80$ Torr (to achieve the condition $v_{Ox} < 0.2v_{Cl}$) were plotted (Fig. 5) according to eqn. (XXXXVIII). The intercept yields

$$k_t/k_3^2 = 2.07 \times 10^{-3} \text{ mol l}^{-1} \text{ s} \qquad \text{(IL)}$$

The ratio $[Cl_2]/[CHCl_3]$ for these experiments ranges between 0.26 and 0.89 and thus the value of k_t/k_3^2 calculated from ref. 18 ranges between 2.14×10^{-3} and 2.39×10^{-3} mol l^{-1} s. The value of eqn. (IL) therefore is in very good agreement with the value obtained previously from the study of the uninhibited photochlorination.

From the experimental points on Fig. 5 it can be seen that the $[O_2]^2$ term in eqn. (XXXXVIII) is negligible under the present experimental conditions and thus

$$k_{10}k_9/k_{-9}k_3^2 = 0.98 \text{ s} \qquad \text{(L)}$$

From the known value of k_3 [18]

$$k_{10}k_9/k_{-9} = 2.2 \times 10^{12} \text{ mol}^{-2} \text{ l}^2 \text{ s}^{-1} \qquad \text{(LI)}$$

can be obtained at 426 K.

For these higher chloroform and lower oxygen pressures the experimental data can be described by the chain terminations (7), (8) and (10). When the oxygen pressure increases, chain termination (11) becomes more important. From the known values [18] of $k_7/k_2'k_3$ and k_8/k_3^2, the values of $(I_a[Cl_2]^2/v_{Cl}^2 - k_t/k_3^2)/[O_2]$ can be calculated as a function of the O_2 concentration. This is shown in Fig. 6 for all the experiments at $P_{CHCl_3} >$

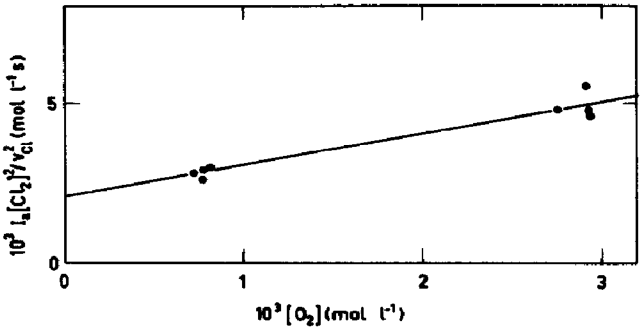

Fig. 5. The oxygen-inhibited photochlorination of chloroform at 426 K: experiments at $P_{CHCl_3} > 150$ Torr and $P_{O_2} < 80$ Torr.

150 Torr. From the intercept and slope of the straight line in this figure, taking into account eqn. (XXXXVIII) and the known value of k_8' [18],

$$k_{10}k_9/k_{-9} = 1.4 \times 10^{12}\ \text{mol}^{-2}\ \text{l}^2\ \text{s}^{-1} \tag{LII}$$

in satisfactory agreement with eqn. (LI), and

$$k_{11}k_9{}^2/k_{-9}{}^2 = 2.8 \times 10^{14}\ \text{mol}^{-3}\ \text{l}^3\ \text{s}^{-1} \tag{LIII}$$

are obtained. It must be pointed out that eqn. (XXXXVIII) does not apply rigorously for all the experiments plotted on Fig. 6, since for some of them v_{Ox} is not negligible. Therefore, the values of eqns. (LII) and (LIII) must be considered as less reliable. For the experiments performed with less than 150 Torr of chloroform the oxidation rates were never negligible compared with the chlorination rates. Under these conditions it is not possible to write a rate equation for the inhibited chlorination taking into account all five chain terminations (7), (8), (10), (11) and (16).

4.3. Combined photochlorination and oxidation data at 426 K

Because of the occurrence of five different chain-terminating steps it is not possible to describe completely the kinetics of this system. The only point that can be verified is the complete reversibility of reaction (9), *i.e.*

$$k_9[CCl_3^{\bullet}]\,[O_2] = k_{-9}[CCl_3O_2^{\bullet}] \tag{LIV}$$

Taking into account eqns. (XXXV) and (XXXVI), eqn. (LIV) becomes

$$v_{Cl}/v_{Ox}{}^{1/2} = \{k_{-9}k_3/k_9(2k_{12})^{1/2}\}[Cl_2]/[O_2] \tag{LV}$$

whatever the chain terminations are. This is shown in Fig. 7, the slope of which yields a value

$$k_{-9}k_3/k_9(2k_{12})^{1/2} = 2.1 \times 10^{-3}\ \text{mol}^{1/2}\ \text{l}^{-1/2}\ \text{s}^{-1/2} \tag{LVI}$$

and from the known value of k_3 [18]

$$k_{-9}/k_9k_{12}{}^{1/2} = 2.0 \times 10^{-9}\ \text{mol}^{3/2}\ \text{l}^{-3/2}\ \text{s}^{1/2} \tag{LVII}$$

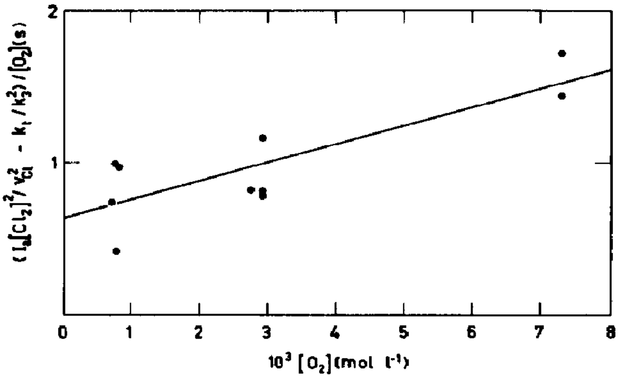

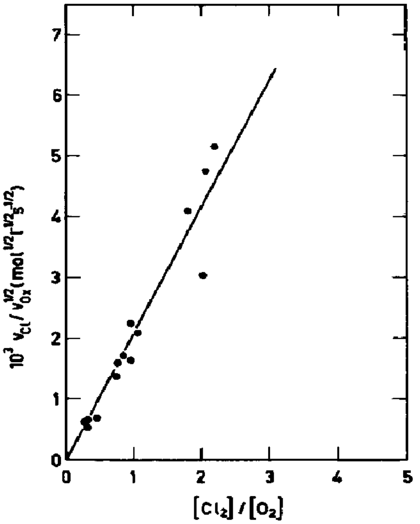

Fig. 6. The oxygen-inhibited photochlorination of chloroform at 426 K: experiments at $P_{CHCl_3} > 150$ Torr.

Fig. 7. The oxygen-inhibited photochlorination and the chlorine-induced oxidation of chloroform at 426 K.

A similar plot for the data at 400 K yields a value

$$k_{-9}/k_9k_{12}^{1/2} = 3.5 \times 10^{-10}\ \text{mol}^{3/2}\ \text{l}^{-3/2}\ \text{s}^{1/2} \qquad \text{(LVIII)}$$

in very good agreement with the combined values of eqns. (XXVI) and (XXIX).

A value

$$k_{11}/k_{12} = 1.1 \times 10^{-3} \qquad \text{(LIX)}$$

can be obtained at 426 K from a combination of eqns. (LIII) and (LVII).

5. General conclusions

The chlorine-photosensitized oxidation and the oxygen-inhibited photochlorination of chloroform can be described by the general mechanism previously proposed for chlorinated ethanes and ethylenes with an additional chain-terminating step

$$CCl_3O_2^{\cdot} + Cl^{\cdot} \xrightarrow{(16)} \text{Products}$$

We would like to emphasize once more the most important point in this mechanism, *i.e.* the biradicalar chain-propagating step for the oxidation (step (12)), the introduction of which is necessary to explain the different reaction orders of the chlorination ($n = \frac{1}{2}$) and the simultaneous oxidation ($n = 1$) against absorbed light intensity.

TABLE 6

Measured complex rate constants

Constants	*Rate constant values*				*Arrhenius equation* $\log_{10} k$
	$T = 303$ K	$T = 346$ K	$T = 400$ K	$T = 426$ K	
$k_{10}k_9/k_{-9}$ ($\mathrm{mol}^{-2}\,\mathrm{l}^2\,\mathrm{s}^{-1}$)			1.0×10^{13}	2.2×10^{12} 1.4×10^{12}	$0.65 + 22\,600/458T$
$k_{11}k_9^{\,2}/k_{-9}^{\,2}$ ($\mathrm{mol}^{-3}\,\mathrm{l}^3\,\mathrm{s}^{-1}$)			6.0×10^{15}	2.8×10^{14}	$-5.97 + 39\,800/4.58T$
$k_{10}k_{-9}/k_{12}k_9$ ($\mathrm{mol\,l}^{-1}$)			1.2×10^{-6}		
$k_{-9}/k_9k_{12}^{\,1/2}$ ($\mathrm{mol}^{3/2}\,\mathrm{l}^{-3/2}\,\mathrm{s}^{1/2}$)			3.5×10^{-10}	2.0×10^{-9}	$2.91 - 22\,600/4.58T$
k_{11}/k_{12}	3.4×10^{-3} 3.2×10^{-3}	2.2×10^{-3} 1.7×10^{-3}	1.5×10^{-3} 1.3×10^{-3}	1.1×10^{-3}	$-4.07 + 2200/4.58T$
$k_{16}/k_{12}^{\,1/2}$ ($\mathrm{mol}^{-1/2}\,\mathrm{l}^{1/2}\,\mathrm{s}^{-1/2}$)	4.1×10^4	6.1×10^4	4.5×10^4		$4.84 - 200/4.58T$

Many complex rate constants were estimated at the four temperatures. They are summarized in Table 6. From this table it appears that the only rate constant involving an important activation energy is k_{-9} with E_{-9} = 22 kcal mol^{-1}. Rate constant k_{12} could have an activation energy of up to 2 kcal mol^{-1}. Considering the confidence limits of the measured rate constants, a value $k_{11}/k_{12} = 2 \times 10^{-3}$ independent of temperature is not excluded. The values

$$\log_{10}(k_{-9}/k_9)\ (\text{mol l}^{-1}) = 22000/4.58T + 9.0$$

$$\log_{10}k_{10}\quad (\text{mol}^{-1}\ \text{l s}^{-1}) = 9.2$$

$$\log_{10}k_{11}\quad (\text{mol}^{-1}\ \text{l s}^{-1}) = 8.0$$

$$\log_{10}k_{12}\quad (\text{mol}^{-1}\ \text{l s}^{-1}) = 10.7$$

$$\log_{10}k_{16}\quad (\text{mol}^{-1}\ \text{l s}^{-1}) = 10.1$$

are, within experimental error, compatible with the data of Table 6. Furthermore, their values are close to those estimated previously [3 - 10] for similar constants for chloroethanes and chloroethylenes.

Acknowledgments

The author wishes to thank L. Bertrand, G. Huybrechts, L. Meyers-Exteen and I. Skibida who performed some preliminary experiments on this system more than 10 years ago. Most of the experiments at 303 K were performed by J. C. van Craen as final research work for his Mémoire de Licence. The author is also indebted to G. R. de Mare for critical reading of this manuscript. Thanks are also due to the Fonds E. Defay for financial support.

References

1 E. Sanhueza, *J. Photochem.*, *7* (1977) 325.
2 H. J. Schumacher, *J. Photochem.*, *9* (1978) 495.
3 G. Huybrechts, G. Martens, L. Meyers, J. Olbregts and K. Thomas, *Trans. Faraday Soc.*, *61* (1965) 1921.
4 P. Goldfinger, G. Huybrechts, G. Martens, L. Meyers and J. Olbregts, *Trans. Faraday Soc.*, *61* (1965) 1933.
5 G. Huybrechts and L. Meyers, *Trans. Faraday Soc.*, *62* (1966) 2191.
6 G. Huybrechts, J. Olbregts and K. Thomas, *Trans. Faraday Soc.*, *63* (1967) 1647.
7 L. Bertrand, J. A. Franklin, P. Goldfinger and G. Huybrechts, *J. Phys. Chem.*, *72* (1968) 3926.
8 L. Bertrand, L. Exsteen-Meyers, J. A. Franklin, G. Huybrechts and J. Olbregts, *Int. J. Chem. Kinet.*, *3* (1971) 89.
9 L. Bertrand, J. Bizongwako, G. Huybrechts and J. Olbregts, *Bull. Soc. Chim. Belg.*, *81* (1972) 73.

10 D. Gillotay and J. Olbregts, *Int. J. Chem. Kinet.*, *8* (1976) 11.

11 P. Goldfinger and G. Huybrechts, *Chemical Kinetics and Chain Reactions*, Nauka, Moscow, 1966, p. 323.

12 H. J. Schumacher and K. Wolff, *Z. Phys. Chem., Abt. B*, *26* (1934) 453.

13 J. H. Knox, *Trans. Faraday Soc.*, *58* (1962) 275.
P. G. Ashmore and M. S. Spencer, *Trans. Faraday Soc.*, *60* (1964) 1608.
P. Goldfinger, G. Huybrechts and G. Martens, *Trans. Faraday Soc.*, *57* (1961) 2210.

14 P. B. Ayscough, A. J. Cocker, F. S. Dainton and S. Hirst, *Trans. Faraday Soc.*, *58* (1962) 295.

15 P. G. Ashmore, B. P. Levitt and B. A. Thrush, *Trans. Faraday Soc.*, *52* (1956) 830.

16 G. Chiltz, S. Dusoleil, P. Goldfinger, G. Huybrechts, A. M. Mahieu, G. Martens and D. Van der Auwera, *Bull. Soc. Chim. Belg.*, *68* (1959) 5.

17 J. C. Olsen, G. E. Ferguson, V. J. Sabetta and L. Scheflan, *Ind. Eng. Chem.*, *3* (1931) 189.

18 G. R. De Maré and G. Huybrechts, *Trans. Faraday Soc.*, *64* (1968) 1311.